Supporting Information

The HLTF HIRAN domain positions the DNA translocase motor to drive efficient DNA fork regression

Diana A. Chavez, Briana H. Greer, and Brandt F. Eichman

Table S1. Oligodeoxynucleotides used in this study			
Substrate	**Name**	**Length**	**Sequence (5′-3′)** [a]
EMSA & footprinting			
	ov_F	30	^{32}P-TTTTTTTTTTTTTTTCCGCTACGCATGTCC-FAM
	ov_0	15	GGACATGCGTAGCGG
	ov_1	16	GGACATGCGTAGCGGT
	ov_2	17	GGACATGCGTAGCGGTT
	ov_3	18	GGACATGCGTAGCGGTTT
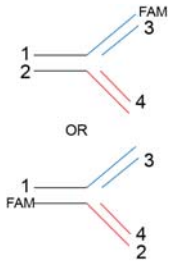	1_F	55	GCATCCGACTCAGTTCGCTCGAGCTAGCCCTGATATCGATGGATCTAGAGCTACC-FAM
	1	55	GCATCCGACTCAGTTCGCTCGAGCTAGCCCTGATATCGATGGATCTAGAGCTACC
	2	55	GGCGAAGGGATCCGTAGGCACAGTTCCCCTAGCTCGAGCGAACTGAGTCGGATGC
	2_F	55	GGCGAAGGGATCCGTAGGCACAGTTCCCCTAGCTCGAGCGAACTGAGTCGGATGC-FAM
	3	28	GGTAGCTCTAGATCCATCGATATCAGGG
	3_TT	28	GGTAGCTCTAGATCCATCGATATCAGTT
	3_PO4	28	GGTAGCTCTAGATCCATCGATATCAGTT-PO_4
	3gap_TT	19	GGTAGCTCTAGATCCATTT
	4	28	GGGAACTGTGCCTACGGATCCCTTCGCC
Fork regression			
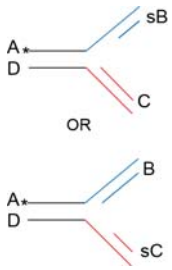	A	122	^{32}P-CGTGACTTGATGTTAACCCTAACCCTAAGATATCGCGTTATCAGAGTGTGAGGATACATGTAGGCAATTGCCACGTGTCTATCAGCTGAAGTTGTTCGCGACGTGCGATCGTCGCTGCGACG
	B	82	CGTCGCAGCGACGATCGCACGTCGCGAACAACTTCAGCTGATAGACACGTGGCAATTGCCTACATGTATCCTCACACTCTGA
	C	82	TCAGAGTGTGAGGATACATGTAGGCAATTGCCACGTGTCTATCAGCTGAAGTTGTTCGCGACGTGCGATCGTCGCTGCGACG
	D	122	CGTCGCAGCGACGATCGCACGTCGCGAACAACTTCAGCTGATAGACACGTGGCAATTGCCTACATGTATCCTCACACTCTGAATACGCGATATCTTAGGGTTAGGGTTAACATCAAGTCACG
	sB	52	CGTCGCAGCGACGATCGCACGTCGCGAACAACTTCAGCTGATAGACACGTGG
	sC	52	CCACGTGTCTATCAGCTGAAGTTGTTCGCGACGTGCGATCGTCGCTGCGACG
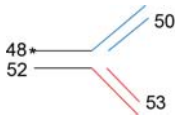	48	60	^{32}P-ACGCTGCCGAATTCTACCAGTGCCTTGCTAGGACATCTTTGCCCACCTGCAGGTTCACCC
	50	30	GGGTGAACCTGCAGGTGGGCAAAGATGTCC
	50-GG	30	GGGTGAACCTGCAGGTGGGCAAAGATGTGG
	52	60	GGGTGAACCTGCAGGTGGGCAAAGATGTCCCAGCAAGGCACTGGTAGAATTCGGCAGCGTC
	53	30	GGACATCTTTGCCCACCTGCAGGTTCACCC

Fork restoration

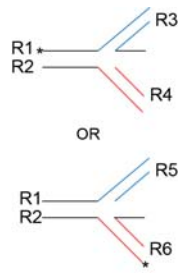	R1	62	(32P-)TAGGCAATTGCCACGTGTCTATCAGCTGAAGTACAAGCGCTGCACCCTAGGTCCGACGCTGC
	R2	62	(32P-)CGTCGCAGCCTGGATCCCACGTCGCGAACAACTTCAGCTGATAGACACGTGGCAATTGCCTA
	R3	62	GCAGCGTCGGACCTAGGGTGCAGCGCTTGTTGTTCAGGTGATACACACGCGGCAAATGCCTA
	R4	30	TGTTCGCGACGTGGGATCCAGGCTGCGACG
	R5	30	GCAGCGTCGGACCTAGGGTGCAGCGCTTGT
	R6	62	TAGGCATTTGCCGCGTGTGTATCACCTGAACATGTTCGCGACGTGGGATCCAGGCTGCGACG

ATPase assays

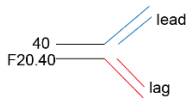	40	40	CTCAGGACTCAGTTCGTCAGCCCTTGACAGCGATGGAAGC
	Lead	20	GCTTCCATCGCTGTCAAGGG
	Lag	20	GGGAACTGTCGCTACCTTCG
	F20.40	40	CGAAGGTAGCGACAGTTCCCCTGACGAACTGAGTCCTGAG

[a] Underlined nucleotides form mismatched base pairs

[b] Sequences for the *ABCD*-type fork regression and fork restoration substrates were taken from Bétous *et al* (2013) *Cell Reports*, 3: *1958-69.*

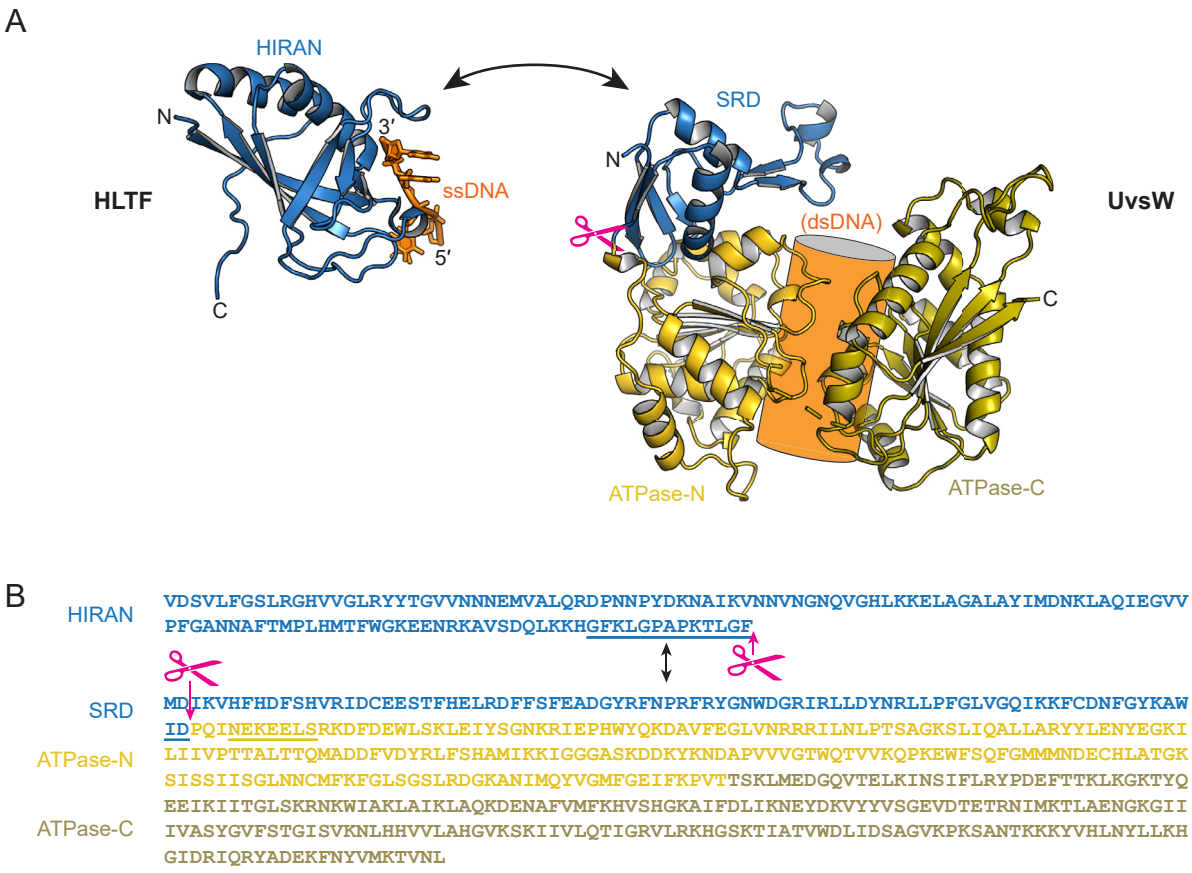

Fig S1. Details of the HIRAN-UvsW chimera. **A**. Crystal structures of HLTF HIRAN domain (PDB ID 4S0N) and UvsW (PDB ID 2OCA). Substrate recognition domain (SRD) and ATPase motor are colored blue and gold, respectively, and DNA is colored orange. The orange cylinder behind UvsW denotes the predicted position of duplex DNA bound to the motor domain based on other superfamily 2 helicase structures. To make the chimera, the UvsW SRD was replaced by HIRAN at the location indicated by the magenta scissors. The C-terminus of the HIRAN domain contains a 13-residue random coil after the last secondary structure element. **B**. Amino acid sequences of the structures shown in panel A. Splice points are marked by the magenta scissors. Random coil sequences around the splice points are underlined.

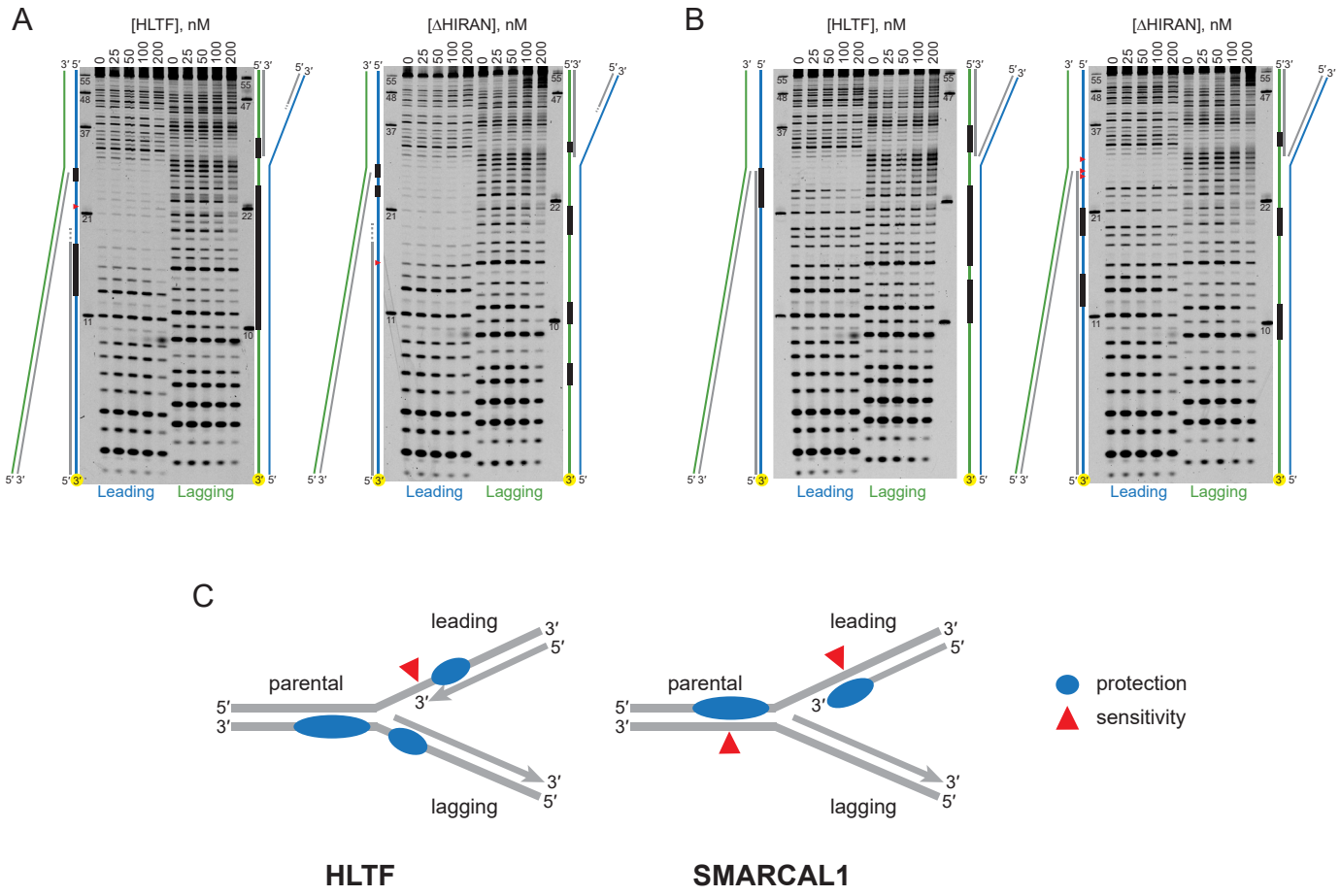

Fig S2. DNase footprinting data. **A**,**B**. Representative gels for wild-type and ΔHIRAN HLTF binding to gapped (A) and non-gapped (B) forks. Either the leading template (left sides of gels) or the lagging template (right sides) strand was labeled with fluorescein, indicated by the yellow circle in the DNA schematics. DNA concentration was held fixed at 100 nM. Lanes represent increasing concentrations of HLTF. Only 0 and 200 nM HLTF lanes were used in quantification shown in Fig. 4. Molecular weight markers are in the outermost lanes and are labeled as the number of nucleotides. Black bars and red triangles on the DNA schematics represent nuclease protected and sensitive regions, respectively. C. Differences in DNase footprinting by HLTF and SMARCAL1 (ref: Bétous et al (2013) Cell Reports, 3: 1958-69).

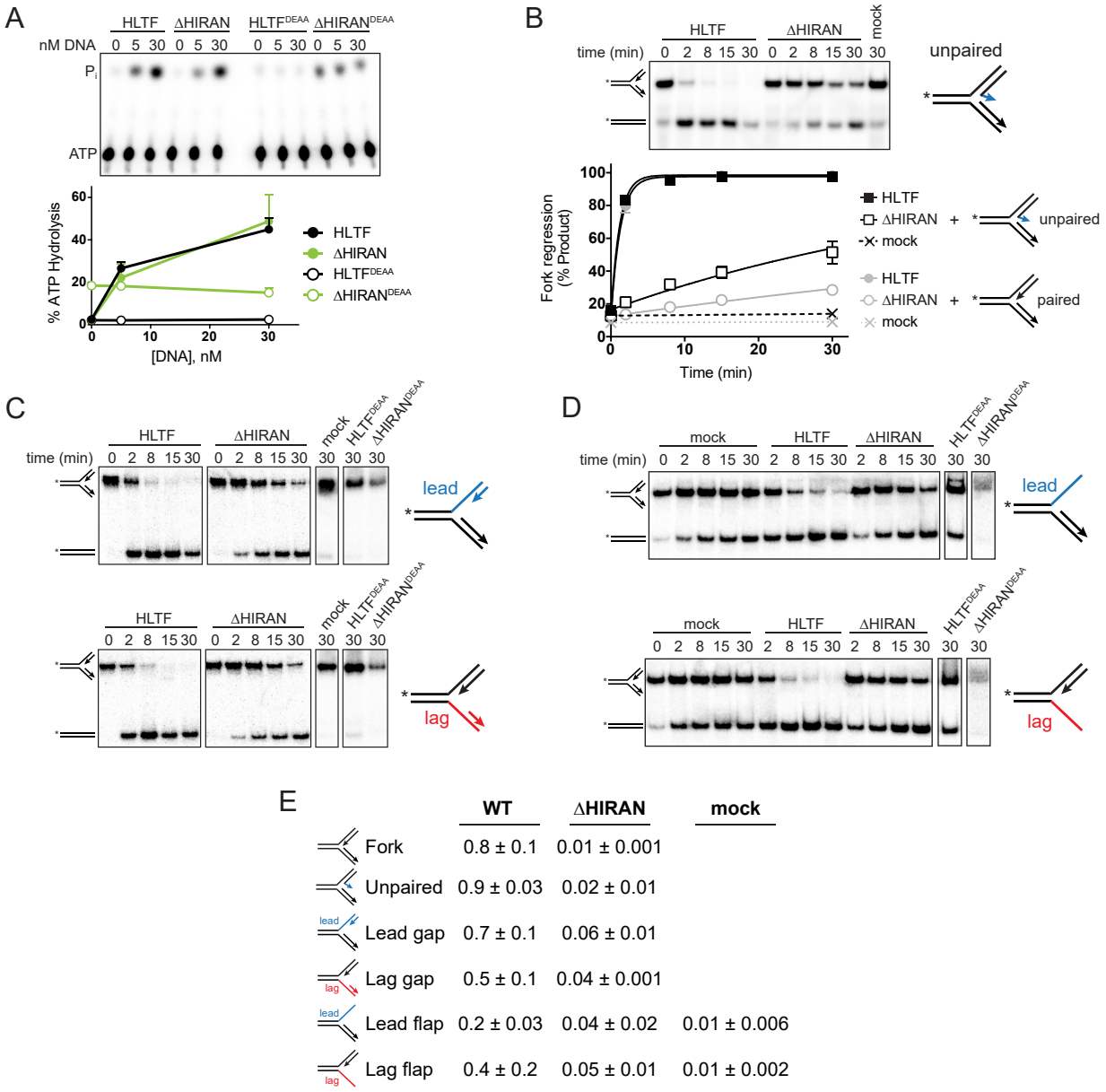

E

	WT	ΔHIRAN	mock
Fork	0.8 ± 0.1	0.01 ± 0.001	
Unpaired	0.9 ± 0.03	0.02 ± 0.01	
Lead gap	0.7 ± 0.1	0.06 ± 0.01	
Lag gap	0.5 ± 0.1	0.04 ± 0.001	
Lead flap	0.2 ± 0.03	0.04 ± 0.02	0.01 ± 0.006
Lag flap	0.4 ± 0.2	0.05 ± 0.01	0.01 ± 0.002

Fig S3. ATPase and fork regression activities of ΔHIRAN. **A**. Left, representative ATPase activities of HLTF, ΔHIRAN, or D557A/E558A mutants of each (HLTF^{DEAA}, ΔHIRAN^{DEAA}) in the presence of fork DNA. Shown is the phosphorimage of TLC plates containing ^{32}P-γATP substrate and inorganic ^{32}P product. Right, quantification of data (average ± S.D.) from three independent measurements. The ΔHIRAN^{DEAA} preparation shows a contaminating ATPase activity not stimulated by DNA. **B**. Left, representative native gel of time-dependent regression by HLTF and ΔHIRAN of a fork containing 2 mismatched base-pairs at the 3′-end of the nascent leading strand. Right, quantification of data (average ± S.D.) from three independent measurements. Regression of the fully base-paired fork is shown in grey for comparison. **C**,**D**. Representative native gels of time-dependent fork regression by HLTF and ΔHIRAN using forks in which the leading or lagging nascent strands have been shortened (C) or removed (D). Endpoints of reactions containing ATPase-dead HLTF^{DEAA} or ΔHIRAN^{DEAA} proteins, or of a mock reaction with no protein are shown as negative controls. Quantification of data is shown in Fig. 5C and 5D. The 40% weaker DNA signal in the ΔHIRAN^{DEAA} lanes are the result of a contaminating nuclease activity in that protein preparation. **E**. Rates of fork regression (min^{-1}) derived from exponential fits to the data shown in Fig. 5 and Fig. S2B-D. Values are average ± S.D., n=3.

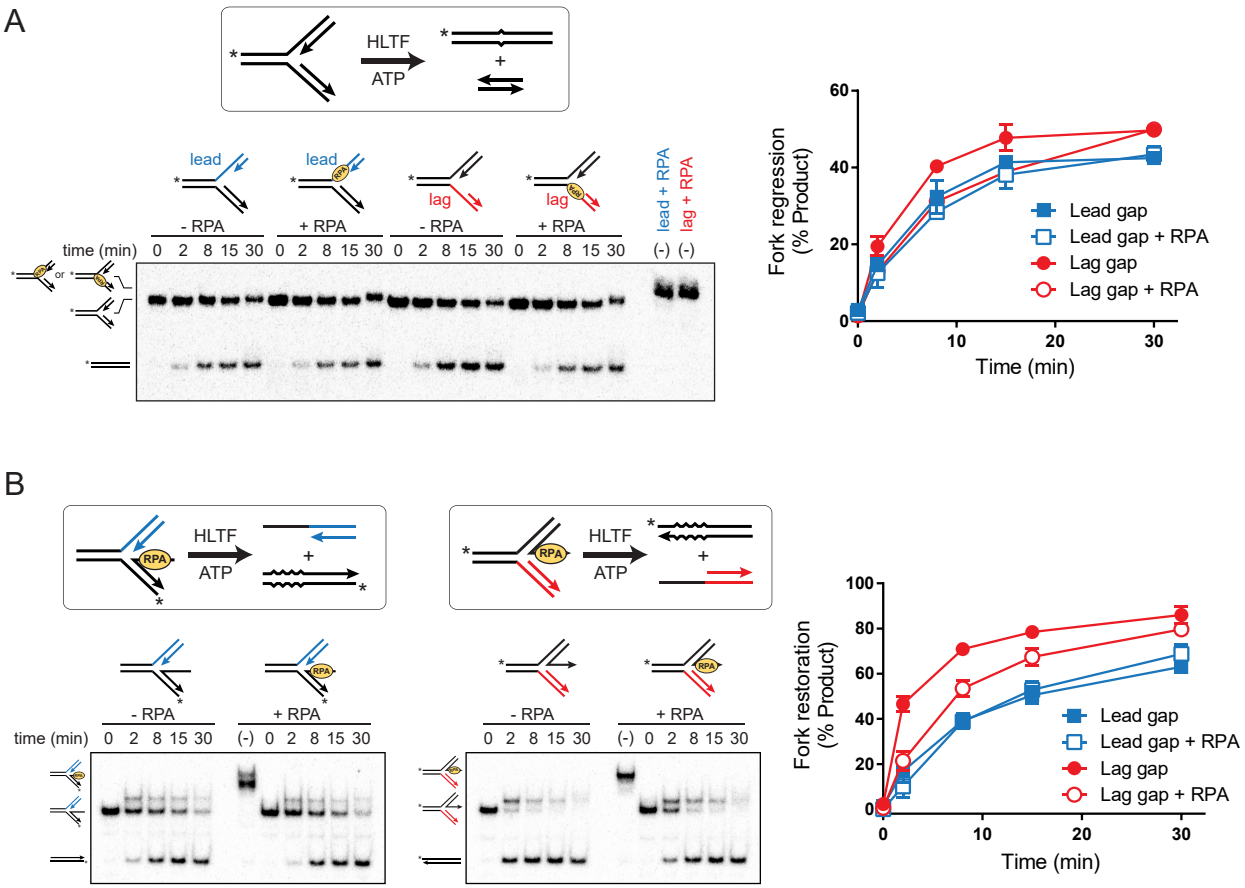

C

	Reversal		Restoration	
	-RPA	+RPA	-RPA	+RPA
HLTF	No preference	Inhibits lag gap	Lag gap	Inhibits lag gap
SMARCAL1	Lag gap	Lead gap	No preference	Lag gap
ZRANB3	No preference	Inhibits lead gap	Lag gap	Inhibits lag gap

Fig S4. Effects of RPA on fork remodeling activities. **A**,**B**. Fork regression (A) and restoration (B) by HLTF. Fork substrates contain 30-nucleotide ssDNA regions on either the template (A) or nascent strands (B) that are bound by RPA. Experimental details are as specified in Experimental Procedures, except DNA was pre-incubated with 3 nM RPA for 30 min prior to addition of HLTF. Representative native gels show ratios of substrates and products over time. The samples lanes labeled "(-)" were not treated with proteinase K prior to loading to verify RPA was bound to the substrates under the experimental conditions. The plots show average data from three experiments (mean ± S.D.). **C**. Comparison of effects of RPA on fork reversal and restoration of HLTF, SMARCAL1, and ZRANB3. Preferences for either leading or lagging gap substrates are specified. Data for SMARCAL1 and HLTF are summarized from data reported in Bétous *et al* (2013) *Cell Rep*, 3: 1958-69.